Window Effects in Zeolite Diffusion and Brownian Motion over Potential Barriers

Johannes M. Nitsche
Dept. of Chemical Engineering, State University of New York, Buffalo, NY 14260

James Wei
Dept. of Chemical Engineering, Massachusetts Institute of Technology, Cambridge, MA 02139

Gorring (1973) reported a phenomenon, the "window effect," whereby the diffusivities of normal paraffins within zeolite T do not decrease monotonically with increasing carbon number N, as would be expected intuitively. Rather, following an initial decrease with N, the diffusivities exhibit a local minimum at C8 followed by a pronounced local maximum at C12. This article presents a theoretical analysis of the window effect and related phenomena, based on an analogy of the configurational diffusion process with an "equivalent" one-dimensional Brownian motion of a rod through a periodic sequence of potential barriers. Numerical calculations are found to be in reasonable agreement with Gorring's experimental data and quantify his qualitatively-stated mechanism, namely that n-alkanes longer than C8 are too large to fit entirely within the potential wells formed by erionite cages and therefore experience smaller energetic barriers to diffusion.

Introduction

Zeolites and related materials find wide industrial use as highly selective catalysts and sorptive separators. Important applications include: cracking of gas oil, conversion of methanol to gasoline, dewaxing of lubricating oils, and separation of *n*-paraffins (Breck, 1974; Barrer, 1978, 1984; Weisz, 1980). In all these processes, diffusion of hydrocarbons through crystalline structures with micropores of molecular dimensions, that is, configurational diffusion (Weisz, 1973), plays a key role. Whereas Brownian motion within fluid-filled pores (Deen, 1987) and Knudsen diffusion (Kennard, 1938) are both reasonably well-understood processes, many aspects of the configurational regime represent open problems. Progress toward the fundamental understanding of this latter mode of diffusive transport will be of value to the design and detailed modeling of commercially important catalysis and sorption processes.

In this article we seek to quantitatively model a now well-known (and, on reflection, quite remarkable) observation reported by Gorring (1973), who measured diffusivities of *n*-alkanes C2 through C14 (and some additional compounds) in zeolite *T* via gravimetric analysis of transient uptake. Initially, the effective diffusivity decreases more or less monotonically with increasing carbon number *N*, in agreement with intuition, but surprisingly, it then passes through a local minimum at C8 followed by a pronounced local maximum at C12; indeed, the diffusivity of C12 is found to exceed that of C8 by a factor of about 140. Based on molecular and crystalline structural dimensions, Gorring's qualitative explanation for this curious transport phenomenon [which is consistent with previously measured product distributions for cracking of normal paraffins (Chen et al., 1969)] involves the observation that C9 and longer *n*-alkanes are too large to "fit" entirely within the energetic potential wells formed by the zeolite cages, and therefore effectively experience variations in potential energy of smaller amplitude (i.e., *lower* potential *barriers*) than does C8. In their discussion of "resonant diffusion," Ruckenstein and Lee (1976) use general symmetry arguments to establish that window effects should, in fact, occur whenever the length of the diffusing molecule is an integral multiple of the pertinent period of the host lattice, as discussed later. Within the present context, this makes it conceivable that experiments of the type carried out by Gorring (1973) but with longer aliphatic chains might exhibit further window effects, the next maximum being expected near carbon number $N=24$. The window effect has also been rationalized recently by Derouane et al. (1988) in

terms of the effects of wall curvature upon the van der Waals interaction between the diffusing molecule and molecular-scale confining pore walls, with some success.

Here, we develop a simple one-dimensional model for the configurational diffusion process, closely aligned with the views expressed by Gorring (1973) and Ruckenstein and Lee (1976), via exploitation of analogies with an "equivalent" Brownian motion of a particle in a periodic potential. Detailed theoretical analysis leads to a description of the window effect in terms of key physical parameters and corroborates Gorring's basic mechanism with some clarification. The following two sections describe our Brownian model in general terms and introduce requisite results from the theory of effective transport. These developments are applied first to a preliminary illustrative calculation and subsequently to a semiquantitative model predicated on details of zeolite structure. The relative importance of various possible diffusion paths is also considered.

A Brownian Motion Model

Gorring (1973) and others (e.g., Chen et al., 1969; Breck, 1974) have given detailed descriptions of pertinent zeolite structures, which take the form of complex lattices characterizable in gross terms as periodic arrays of "cages" or pore bodies interconnected by "windows" or throats, as discussed in greater detail later on. Configurational diffusion of relatively tightly fitting hydrocarbons through such lattices differs significantly from corresponding transport processes occurring within *fluid-filled* pores (Deen, 1987), in that there is insufficient space for the interposition of small solvent molecules between solute and pore walls. Nevertheless, an analogy exists between these two distinct processes, because thermal vibrations of the lattice introduce a stochastic element into the otherwise deterministic trajectory of the hydrocarbon, not unlike that in *Brownian* diffusion, at least in gross terms. Also, complex energetic interactions of the hydrocarbon with the individual atoms making up the zeolite crystal (cf. June et al., 1990) can be characterized approximately and simply in terms of periodically positioned energetic barriers (Riekert, 1970). It is precisely for these sorts of reasons that Brownian diffusion of a particle subjected to the force deriving from a periodic potential Ψ has been used as a model for diffusion (Larsen and Schuss, 1978; Schuss 1980) and superionic conduction (Dieterich et al., 1980) in crystalline solids. In such applications, the diffusion coefficient D must, of course, be regarded as a phenomenological parameter, dependent on vibrational and other properties of the host lattice.

With the preceding considerations in mind, we propose a simple one-dimensional Brownian model for the configurational diffusion of a linear paraffin within a zeolite, Figure 1. The paraffin is identified with a rod-like entity of length L undergoing axial Brownian motion within a constricted capillary. Because of the highly constrained character of its motion, it is reasonable in this approximate formulation to ignore flexibility of the chain. Energetic interactions of the rod with the zeolite are approximated in terms of a periodic potential $\Phi(x')$ (period $= l$) having dimensions of energy per unit of paraffin length. The minima correspond to the wider cages, and the maxima correspond to the narrower windows between cages. As in all diffusion processes involving species of appreciable extent, attention is focused on the position x of a

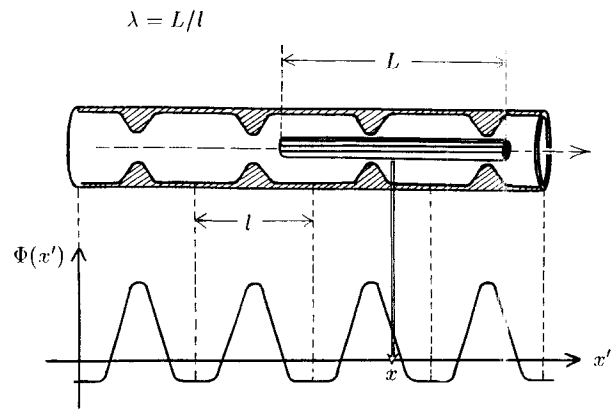

Figure 1. Brownian model for configurational diffusion of an aliphatic chain.

locator point fixed in the rod—the midpoint, say, for definiteness. Then, in the absence of more detailed information, it is assumed that the total potential energy $\Psi(x; L)$ of the rod is simply a superposition of the energies $\Phi(x')dx'$ associated with each linear element dx' at position x':

$$\Psi(x; L) = \int_{x-L/2}^{x+L/2} \Phi(x')dx'. \tag{1}$$

Periodicity of Φ implies periodicity of Ψ.

Under the most general circumstances, the mobility of the paraffin will possess spatial variations. This implies that the pseudodiffusivity D may be a periodic function of position. In any case, D is expected to decrease with increasing chain length L. Given the ambiguities associated with the construction of our Brownian model, we are content to assume for simplicity that D is independent of position and to arbitrarily use the $1/L^2$ scaling derived by de Gennes (1971) for the diffusivities of polymer chains undergoing reptation within gels. Thus, we take

$$D(x; L) \equiv K_D/L^2, \tag{2}$$

with K_D a phenomenological constant. Our justification for this choice is that the precise dependence of D on position and length of the chain is of only secondary importance, and would not likely have order-of-magnitude consequences. The central feature giving rise to the window effect is the presence of periodic spatial variations in the potential, and this, therefore, is the specific focus of our attention.

In summary, for given chain length L, the *actual* configurational diffusivity of a paraffin is identified with the effective diffusivity of a particle undergoing one-dimensional Brownian motion within a viscous continuum characterized by the potential Ψ and diffusivity D respectively given by Eqs. 1 and 2. It is worth noting explicitly that we do not regard our model as a literal descriptor of the inherently three-dimensional configurational diffusion process. Rather, this work represents a rigorous analysis of a simple process that shares a key element with paraffin diffusion in real zeolites: stochastic motion through a regular array of potential barriers. This element alone already leads to the window effect and thus merits detailed investigation. To proceed with quantitative calculations,

it is necessary first to draw upon certain known results on effective diffusion processes.

Diffusion in Periodic Potentials

Diffusion of a Brownian particle subjected to a spatially periodic force $-\nabla\Psi$ deriving from a periodic potential Ψ has been the subject of considerable scrutiny for many years within a number of physical contexts, including diffusion of ions in polyelectrolyte solutions (Lifson and Jackson, 1962; Jackson and Coriell, 1963; Coriell and Jackson, 1963) and solute transport within biological membranes (Weaver, 1982) in addition to the solid-state applications (Larsen and Schuss, 1978; Schuss, 1980; Dieterich et al., 1980) indicated above. In macroscopic terms, the diffusion process may be characterized by an *effective diffusivity* $\overline{D}$ representing an average property of the periodic microstructure. $\overline{D}$ has significance in terms of both: (1) steady-state solute flux in response to a concentration difference imposed across a large sample (Jackson and Coriell, 1963); and (2) stochastic "spreading" once sufficient time has elapsed for diffusive sampling of the microstructure to occur (Festa and Galleani d'Agliano, 1978; Brenner and Adler, 1982). The key result of pertinence to subsequent developments is the following general formula (Festa and Galleani d'Agliano, 1978) for the one-dimensional case,

$$\overline{D}=\left[l^{-1}\int_0^l \frac{e^{\Psi(x)/kT}}{D(x)}dx\cdot l^{-1}\int_0^l e^{-\Psi(x)/kT}dx\right]^{-1}, \tag{3}$$

which gives $\overline{D}$ as a functional of $\Psi(x)$ and $D(x)$.

For the important special case where D is independent of position, considered here, Eq. 3 reduces to

$$\overline{D}=D\left[l^{-1}\int_0^l e^{\Psi(x)/kT}dx\cdot l^{-1}\int_0^l e^{-\Psi(x)/kT}dx\right]^{-1} \tag{4}$$

(cf. Lifson and Jackson, 1962; Larsen and Schuss, 1978; Weaver, 1982). Application of Schwarz's inequality then shows that, in general, $\overline{D}\leq D$ (Lifson and Jackson, 1962; Festa and Galleani d'Agliano, 1978), so that spatial variations in the potential invariably impede the diffusion process in an average sense.

It is well known (Festa and Galleani d'Agliano, 1978; Weaver, 1982) that in the low-temperature or high-barrier limit [more precisely, when $(\Psi_{max}-\Psi_{min})/kT\gg 1$], Eq. 4 conforms to asymptotic behavior of the Arrhenius form,

$$\overline{D}\sim r(T)\exp(-E_a/kT), \tag{5}$$

characteristic of activated jump diffusion processes. Asymptotic results (Weaver, 1982) for several model potentials indicate that the activation energy E_a equals $\Psi_{max}-\Psi_{min}$ independently of the shape of $\Psi(x)$; however, the precise form of the pre-exponential factor $r(T)$ varies with the functional form selected for $\Psi(x)$.

An Illustrative Example

Before proceeding with calculations predicated upon details of zeolite structure, it is worthwhile to consider a simple hypothetical situation that illustrates, in qualitative terms, the window effect and related important phenomena. Attention in this section is, therefore, focused on the special case where the potential energy per unit chain length $\Phi(x')$ is expressible as the sum of sinusoidally varying and constant contributions,

$$\Phi(x')=(A/2)\sin(2\pi x'/l)+A', \tag{6}$$

with A the variation, l the period and A' the additive "background potential." Substitution into Eq. 1 yields the explicit expression

$$\Psi(x)/kT=(2\pi)^{-1}H\sin(\pi\lambda)\sin(2\pi x/l)+\lambda H' \tag{7}$$

for the potential energy of a chain with center at x, where

$$\lambda=L/l \tag{8}$$

is the ratio of the chain length to the period of the potential, and

$$H=Al/kT,\ H'=A'l/kT \tag{9}$$

are dimensionless forms of the barrier height and additive constant potential, respectively. We shall see in a different case below that $H\cong 30$ corresponds very roughly to an activation energy of about 40 kJ/mol for medium-length chains.

It is evident from the amplitude factor $\sin(\pi\lambda)$ in Eq. 7 that there are no potential barriers [$\sin(\pi\lambda)=0$] for $\lambda=1,2,3,\ldots$, because for these values the chain always extends over an integral number of periods no matter what its position, which renders its potential energy independent of x. Thus, at integral values of λ the diffusion process proceeds unimpeded by barriers, and the effective diffusivity exhibits corresponding local maxima. This is the origin of the window effect, as noted generally by Ruckenstein and Lee (1976).

Substitution of Eqs. 2 and 7 into the general formula (Eq. 4) leads to the expression

$$\overline{D}l^2/K_D=[\lambda I_0(s)]^{-2} \tag{10}$$

with

$$s=(2\pi)^{-1}H\sin(\pi\lambda), \tag{11}$$

in consequence of a well-known integral representation (Abramowitz and Stegun, 1965) for the modified Bessel function I_0 (cf. Weaver, 1982). Figure 2a shows the dependence of the effective diffusivity on the dimensionless chain length λ and barrier height H. For H large enough, local maxima in $\overline{D}$ occur near integral values of λ, for which there are no potential barriers, as discussed above. (The maxima in $\overline{D}$ are displaced a bit from $\lambda=1,2,3,\ldots$ owing to the extra factor λ^{-2} in Eq. 10, which arises from the decrease in mobility with increasing chain length—cf. Eq. 2.)

Consideration of Figure 2a and Eqs. 10 and 11 points up a conceptually important phenomenon brought out more clearly by Figure 2b. It is quite plain that when the barrier height H is zero, there are no local maxima in $\overline{D}l^2/K_D$, which then exhibits the simple functional dependence λ^{-2}; moreover, for

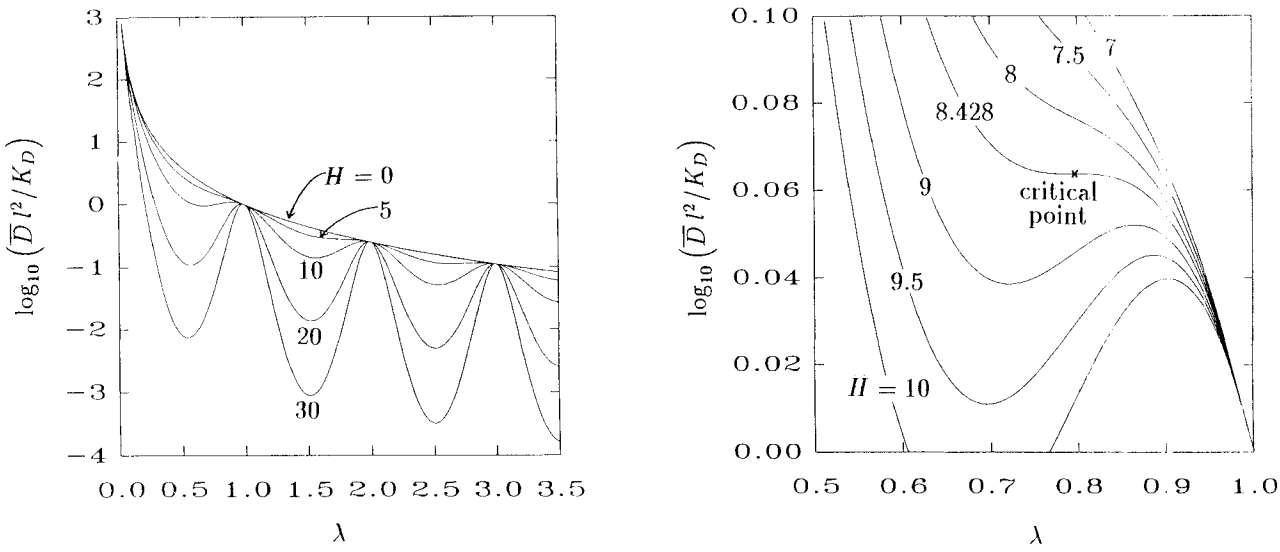

(a) Sequence of window effects *(b) Critical point in the interval $0 < \lambda < 1$*

Figure 2. Dependence of effective diffusivity on dimensionless chain length λ and potential barrier height H for the sinusoidal potential, Eq. 6.

small values of H the potential produces only small deviations from this simple functional form. On the other hand, for larger values of H local maxima exist and can be very pronounced. Thus, for each interval $(i-1, i)$ there must exist a critical value H_i^* of H, below which the dependence of $\overline{D}l^2/K_D$ is monotonic in the interval and above which the window effect occurs. The critical points are determined by the conditions that the first and second derivatives of $\overline{D}l^2/K_D$ with respect to λ vanish, which lead ultimately to the two equations

$$0 = \lambda^{-1} I_0(s) + (H/2)\cos(\pi\lambda) I_1(s), \tag{12}$$

$$0 = [(H^2/4)\cos^2(\pi\lambda) - \lambda^{-2}] I_0(s) + (H/2)[\cos(\pi\lambda)/\lambda - \pi/\sin(\pi\lambda)] I_1(s) \tag{13}$$

in the two variables H and λ. Numerical solution of these equations leads to the coordinates listed in Table 1. The values of H_i^* decrease with i because: (1) critical points arise from the interplay between the monotonic decrease of the diffusivity D with λ and the tendency of the potential to produce local maxima; and (2) the (negative) derivative of D with respect to λ decreases in magnitude as λ increases. Indeed, if the mobility were independent of chain length, then the factor λ^{-2} would be absent in Eq. 10, window effects would occur for all nonzero values of H, and no critical points would exist. Gorring's experiments (1973) correspond to the supercritical regime $H > H_1^*$.

Partitioning

It is immediately apparent from Eqs. 3 and 4 that the effective diffusivity $\overline{D}$ cannot be affected by any x-independent additive contribution to Ψ. In the present case, $\overline{D}$ is independent of the constant "background potential" A' or H', as is evident from the absence of H' from Eqs. 10 and 11. On physical grounds, this energetic parameter is, however, expected to have a significant influence on the diffusive transport process. Where, then, will one see its effect? To answer this question, we note that $\overline{D}$ represents only part of the overall transport picture.

$\overline{D}$ gives the diffusive flux in terms of unit-cell average "solid-phase" concentrations $\overline{C}$ once the alkane is *inside* the heterogeneous ("zeolite") medium. However, given an alkane concentration C_b in a bulk solution phase (with $\Psi \equiv 0$), the equilibrium concentration $\overline{C}$ within an adjacent periodic-potential medium will equal the bulk concentration C_b multiplied by the partition coefficient

$$K = l^{-1}\int_0^l e^{-\Psi(x)/kT} dx. \tag{14}$$

As in the theory of pore diffusion (Deen, 1987, p. 1141), for steady-state situations it is meaningful to absorb the partition coefficient into the effective diffusivity to produce an *overall* diffusivity $\overline{D}_O = K\overline{D}$. This coefficient gives the diffusive flux through a large sample of thickness $x_2 - x_1 \gg l$ in terms of *bulk-phase* solute concentrations, as $-\overline{D}_O(C_{b2} - C_{b1})/(x_2 - x_1)$. For the periodic potential, Eqs. 4 and 14 yield the general integral expression

Table 1. Critical Points (H_i^*, λ_i^*) for the Sinusoidal Potential, Eq. 6

i	λ Interval	H_i^*	λ_i^*
1	(0,1)	8.428	0.796
2	(1,2)	5.458	1.771
3	(2,3)	4.330	2.764
4	(3,4)	3.696	3.760
5	(4,5)	3.278	4.758
.	.	.	.
.	.	.	.
.	.	.	.

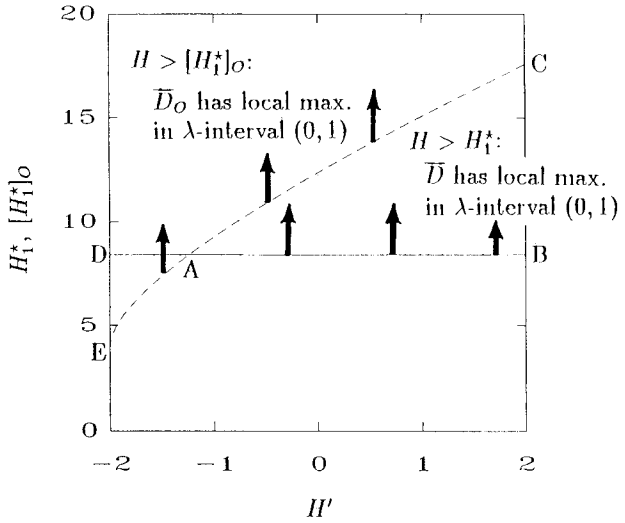

Figure 3. Critical barrier heights above which the effective diffusivity exhibits a local maximum as a function of λ in the interval $0 < \lambda < 1$.

———, H_1^*, corresponds to the effective diffusivity $\overline{D}$; - - - -, $[H_1^*]_O$, corresponds to the *overall* effective diffusivity $\overline{D}_O$, including partitioning effects

$$\overline{D}_O = K\overline{D} = D\left[l^{-1}\int_0^l e^{\Psi(x)/kT}dx\right]^{-1}, \tag{15}$$

applicable to steady-state diffusion, which specializes to

$$\overline{D}_O l^2/K_D = [\lambda^2 e^{\lambda H'} I_0(s)]^{-1} \tag{16}$$

for the sinusoidal-plus-constant potential presently being considered. Whereas $\overline{D}$ depends only on energy differences quantified by H, $\overline{D}_O$ is influenced by the absolute value of the potential (i.e., by how oleophilic or oleophobic the zeolite is) and so is a function of both H and H', as is clear from Eq. 16. Uptake experiments (in particular, Gorring's 1973) measure transient response within the zeolite and therefore give an indication of $\overline{D}$.

It is worth noting that even if $H > H_1^*$, so that a window effect will occur for $\overline{D}$ in the interval $i-1<\lambda<i$, the *overall* diffusivity $\overline{D}_O$ may or may not also exhibit a local maximum depending on the values of the parameters H and H'. This point is brought out by Figure 3, which compares the critical value H_1^* (solid line) of the barrier height H above which $\overline{D}$ goes through a local maximum in the interval $0<\lambda<1$, with corresponding values $[H_1^*]_o$ (dashed curve) for $\overline{D}_O$ as a function of H'. The solid line is horizontal because $\overline{D}$ (and therefore certainly H_1^*) is independent of H'; this line corresponds to the first row in Table 1. The dashed curve is determined numerically from equations analogous to Eqs. 12 and 13 expressing the condition that the first and second derivatives of $\overline{D}_O l^2/K_D$ with respect to λ vanish. In the region bounded by A-B-C where the dashed curve lies above the horizontal solid line, $\overline{D}$ exhibits a window effect but $\overline{D}_O$ does not. Similarly, in the region bounded by A-D-E, $\overline{D}_O$, but not $\overline{D}$, goes through a local maximum. (We note for completeness that the dependence of $\overline{D}_O$ on λ and H undergoes a qualitative change when H' assumes values less than -2. For $H' < -2$, $\overline{D}_O$ ex-

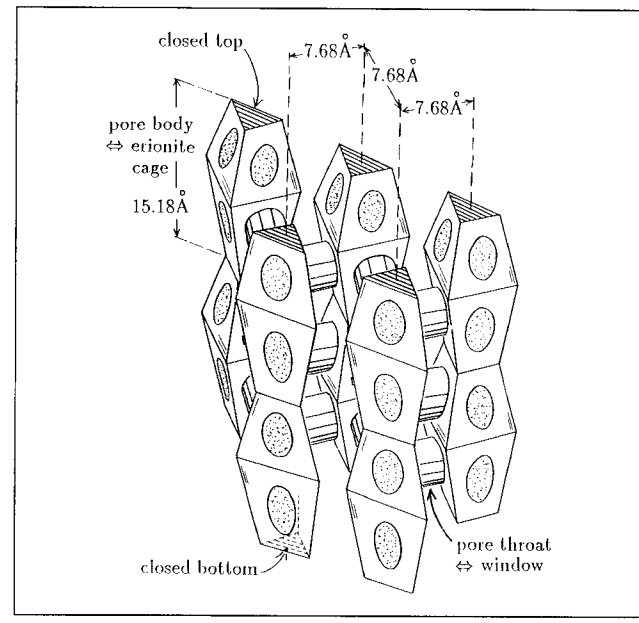

(a) Perspective view of spatial arrangement of erionite cages, idealized as pore "bodies" interconnected by "throats"

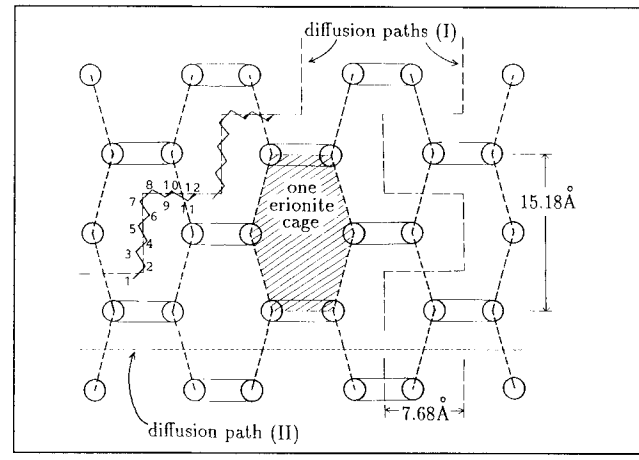

(b) Side view with n-dodecane molecules occupying cages along a diffusion path of type I

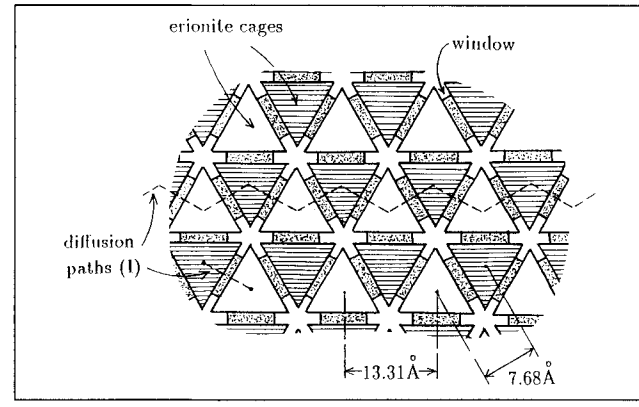

(c) Top view

Figure 4. Structure of erionite.

hibits a local minimum but no local maximum in the interval $0<\lambda<1$ for all H.)

Consideration of Zeolite Structure

As indicated by Gorring (1973), zeolite T is a two-phase composite comprising erionite regions sparsely distributed within a predominantly offretite matrix. Diffusion through offretite is relatively unrestricted compared with erionite. However, diffusion paths are blocked by erionite intergrowths, so that the latter effectively controls the rate of diffusive transport. Until later in this section, attention is therefore focused on erionite.

The detailed structure described by Gorring (1973) can be characterized in terms of a hexagonal array of vertical columns, each composed of pore bodies (erionite cages) stacked one on top of the other, as indicated in Figure 4. Each pore body is connected laterally to six other bodies by energetically unfavorable throats or windows, which are actually eight-membered rings. The tops and bottoms of the bodies are closed off by small six-membered rings, so that transport of paraffins vertically through just a single column of cages is impossible. The free internal height of each cage is approximately 13.0 Å, and the axis-to-axis distance between adjacent columns of cages is 7.68 Å. Gorring's estimates of the dimensions of normal alkanes are based on standard values, a 1.26 Å chain length per C-C bond and a 4.00 Å methyl-group diameter, although the actual contribution of a specific C-C bond to the overall linear extent of a paraffin within the zeolite lattice will, of course, depend on the precise chain conformation. It can be concluded from these dimensions that an aliphatic chain in a conformation alternating between pore bodies and throats (dashed lines labeled I in Figure 4b) will have eight carbon atoms aligned roughly vertically well within a pore body and about four or five leading through each throat.

Assuming zig-zagging diffusion paths (see the dashed lines labeled I in Figures 4b and 4c), it is reasonable to consider a periodic potential for which the period l is identified with carbon number $N=12$. The fact that Gorring found the activation energy for diffusion of tridecane to be zero suggests for l rather $N=13$, and it is likely that 13 carbon atoms could fit within one period of the erionite structure as defined above. However, given the apparent scatter in Gorring's measured activation energies (see his Figures 6–8 and our Figure 6), as well as the ambiguities associated with the present simple model, we will stay with the equivalence $l \Leftrightarrow N=12$, which coincides more neatly with the observed local maximum in the diffusivity at C12.

In the absence of more detailed information, the simplest functional form to consider for $\Phi(x')$ is the periodic step given by

$$\Phi(x') = \begin{cases} 0, & 0<x'<\tau l, \\ A, & \tau l<x'<l, \end{cases} \tag{17}$$

$$\Phi(x'+l) = \Phi(x'), \tag{18}$$

with $0<\tau<1$. The potential wells correspond to the erionite cages (pore bodies), which extend over about eight to ten carbon atoms, so the fraction τ should lie in the interval $8/12 \le \tau \le 10/12$. The corresponding integrated potential $\Psi(x)$

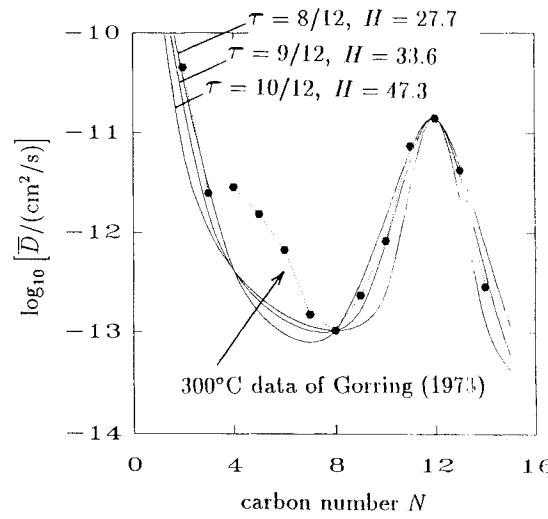

Figure 5. Diffusivities as a function of carbon number *N* for diffusion of *n*-alkanes through zeolite *T*.

Points represent Gorring's (1973) experimental data taken at 300°C (Gorring, 1991). Lines represent calculations based on Eqs. 19–23 for the sets of τ and H indicated in the text. For each value of τ the barrier height H is chosen to reproduce the experimentally observed ratio of diffusivities of C12 to C8, and the calculated diffusivities are scaled to pass through the experimental points for these two paraffins.

given by Eq. 1 is piecewise linear, a fact which allows the integrals in Eq. 4 to be evaluated explicitly, yielding the following expression for the effective diffusivity in the erionite phase:

$$\frac{\overline{D}l^2}{K_D} = \frac{1}{\lambda^2 F_b(\lambda;\tau,H)}, \tag{19}$$

where the function $F_b(\lambda;\tau,H)$ (subscript "b" for "barrier") is given explicitly for $0 \le \lambda \le 1$ by the formulas

$$F_b(\lambda;\tau,H) = \begin{cases} (8/H^2)[\cosh(\lambda H)-1] + (4/H)(1-2\lambda) \\ \sinh(\lambda H) + f(\lambda;\tau)\cosh(\lambda H) + g(\lambda;\tau), \\ \qquad 0 \le \lambda \le 1-\tau, \\ (8/H^2)\{\cosh[(1-\tau)H]-1\} + (4/H)(2\tau-1) \\ \sinh[(1-\tau)H] - f(\lambda;\tau)\cosh[(1-\tau)H] + g(\lambda;\tau), \\ \qquad 1-\tau \le \lambda \le \tau, \\ (8/H^2)\{\cosh[(1-\lambda)H]-1\} + (4/H)(2\lambda-1) \\ \sinh[(1-\lambda)H] + f(\lambda;\tau)\cosh[(1-\lambda)H] + g(\lambda;\tau), \\ \qquad \tau \le \lambda \le 1, \end{cases} \tag{20}$$

in which we make the identification

$$\lambda = (\text{chain length } L)/(\text{period } l) = (\text{carbon number } N)/12. \tag{21}$$

In these equations

$$f(\lambda;\tau) = 2[\tau(1-\tau) - \lambda(1-\lambda)], \tag{22}$$

$$g(\lambda;\tau) = 1 - 2[\tau(1-\tau) + \lambda(1-\lambda)], \tag{23}$$

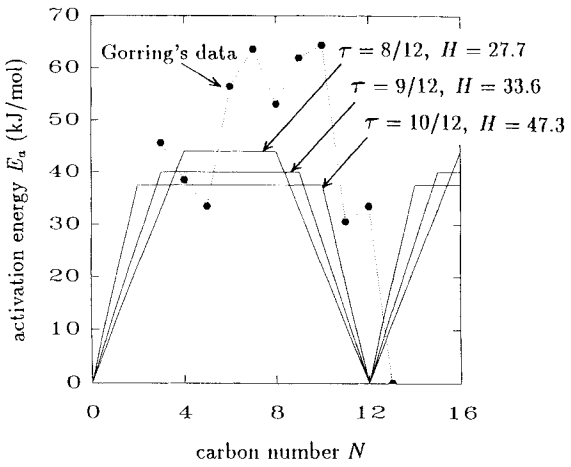

Figure 6. $\Psi_{max} - \Psi_{min}$ as a function of carbon number N.

Comparison of values calculated from Eq. 25 using sets of τ and H listed in the text and Gorring's (1973) measured activation energies.

and, as before, $H = Al/kT$. Some details of the derivation of Eqs. 19-23 are given in Appendix A. It is straightforward to conclude that F_b must be periodic in λ, so that

$$F_b(\lambda + 1;\tau,H) = F_b(\lambda;\tau,H). \tag{24}$$

Equation 19 reproduces the experimentally observed ratio of the diffusivities of C12 to C8 if one takes $H = 27.7$, 33.6 and 47.3 assuming $\tau = 8/12$, 9/12 and 10/12, respectively, as indicated in Figure 5. As shown below, these values lead to activation energies in the model as large as about 40 kJ/mol. It is worth remarking that $H \cong 30$ corresponds to a value of A, the energy per unit chain length parameter, of the order of 12 kJ/mol per CH_2 or CH_3 segment.

Figure 5 represents a superposition of data points from Gorring's Figure 5 (Gorring, 1991) and the predictions of Eqs. 19-23 based on the three sets of values of τ and H, and scaled to pass through the experimental values for C8 and C12. The measured diffusivities of C8 through C14 are reproduced quite well, a finding that supports the present phenomenological approach. However, the "hump" evident in Gorring's data for C4 through C6 or C7 does not appear in our theoretical curve. We note in passing that this "hump" seems to be reproduced by the analysis of Derouane et al. (1988), although for the theoretical curve shown in their Figure 5 it is much more pronounced than even the local maximum at $N = 12$ and is therefore disproportionately large. Whatever the underlying cause of the "hump," it seems to have no representation in our analysis. Considering the simplicity of our one-dimensional periodic-potential model, the overall agreement is quite satisfactory.

It is easily shown (see Appendix A) that $(\Psi_{max} - \Psi_{min})/kT$ is given by

$$(\Psi_{max} - \Psi_{min})/kT = \begin{cases} \lambda H, & 0 \le \lambda \le 1 - \tau, \\ (1-\tau)H, & 1 - \tau \le \lambda \le \tau, \\ (1-\lambda)H, & \tau \le \lambda \le 1. \end{cases} \tag{25}$$

Figure 6 compares $\Psi_{max} - \Psi_{min}$ given by this formula and the previously stated sets of τ and H with the activation energies reported by Gorring [although it must be emphasized that the concept of activation energy does not apply when $(\Psi_{max} - \Psi_{min})/kT \not\gg 1$]. The calculated values are seen to be of the proper order of magnitude.

Two-phase structure of zeolite T

Within the context of our one-dimensional model, zeolite T corresponds to a situation where short intervals of erionite are interspersed between long intervals of offretite. Assuming that the respective intervals contain sufficiently many repetitions of their constituent cages so that each phase may be regarded as a pseudocontinuum [cf. Whitaker (1988) in connection with two-phase media where a "phase" may be heterogenous on a smaller scale], the effective diffusivity $\overline{D}_T$ of zeolite T would be given by

$$\overline{D}_T = \left(\frac{\varphi_e}{\overline{D}_e} + \frac{1 - \varphi_e}{\overline{D}_o} \right)^{-1}, \tag{26}$$

where the subscripts e and o distinguish erionite and offretite, respectively, and φ denotes the volume fraction, in the present case equal to 0.02-0.05 for erionite (Gorring, 1973, p. 16). This resistances-in-series expression is quite appropriate to the real situation because erionite intergrowths have been described as lamellae (Bennett and Gard, 1967). If $\overline{D}_e$ is sufficiently small relative to $\overline{D}_o$, then Eq. 26 suggests that $\overline{D}_T$ will be approximately proportional to $\overline{D}_e$. In the actual physical system, the zig-zagging path would also require a tortuosity correction factor. Whatever the case may be, the preceding analysis still indicates the overall form of the functional dependence of the effective diffusivity on carbon number N, numerical factors aside.

Energetically Unfavorable Alternate Paths

It remains to address one important issue relating to an ambiguity regarding the path along which an aliphatic chain diffuses through erionite. According to the model detailed above, a chain alternates between pore bodies and throats (paths of type I in Figure 4b). Although Gorring regards *n*-octane as occupying the pore bodies vertically (and higher alkanes as occupying the bodies vertically to the extent possible), his discussion of *n*-dodecane (p. 22) seems to indicate that the latter molecule diffuses horizontally through a sequence of only pore throats (see path II in Figure 4b). Chen et al. (1969) and Ruckenstein and Lee (1976) also give this impression. Upon reflection, it becomes apparent that there are, in fact, many paths a chain could take through the erionite structure. The least tortuous (moreover, perhaps highest-mobility) path II of Figure 4b would avoid vertical occupation of the pore bodies altogether in favor of mainly high energy states; the most tortuous path I of Figure 4b would correspond to the zig-zagging assumed here, alternating between low- and high-energy states. Which, if any one, of the possible paths then characterizes the diffusion process? The answer to this question probably has much to do with the potential energies associated with the configurations in question. A molecule following path I tends to minimize its resting potential energy by occupying the pore bodies (potential wells) as much as possible. On physical grounds and in consideration of the

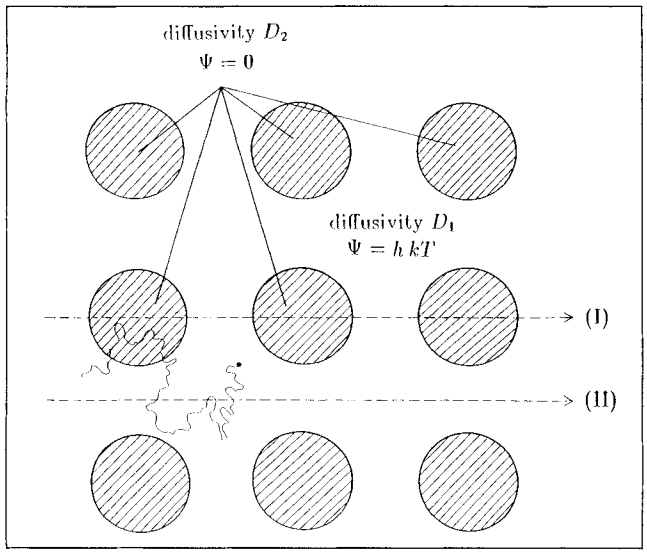

Figure 7. Diffusion of a Brownian point particle in a periodic medium where both its diffusivity and potential energy are piecewise constant.

equilibrium Boltzmann distribution, paths of type I (tacitly assumed in the preceding calculations) are expected to dominate the diffusion process, even though low energy might come at the expense of decreased mobility.

These ideas can be addressed quantitatively in part by considering a different situation: the diffusion of a point-sized particle through the medium depicted in Figure 7. In the circular regions, occupying area fraction φ, the potential Ψ is zero and the diffusivity is D_2. In the surrounding matrix, the potential Ψ equals $h>0$ (measured in units of kT) and the diffusivity is D_1. We consider the case $D_2<D_1$. Path II is devoid of potential barriers (because it proceeds over configurations with uniformly high energy) and is characterized by the higher mobility. In contrast, path I involves motion through (low-energy) potential wells and has the lower overall mobility. As detailed in Appendix B, numerical values for the effective diffusivity in this system can be derived by combining a recent analysis of effective diffusion by Whitaker (1988) and typical numerical results for the effective conductivities of composite materials composed of a matrix with cylindrical inclusions of higher conductivity arranged in a square array (e.g., Perrins et al., 1979). Figure 8 compares these exact effective diffusivities with approximate values calculated from the formulas

$$\overline{D}/D_1 = \{(1-\tau)^2 + (D_1/D_2)\tau^2 + \tau(1-\tau)[\exp(h) + (D_1/D_2)\exp(-h)]\}^{-1}, \quad (27)$$

$$\tau = 2(\varphi/\pi)^{1/2}, \quad (28)$$

derived by applying Eq. 3 to the hypothetical lowest-energy, effectively one-dimensional path I, corresponding to periodic step change in Ψ and D. The lowest energy path yields a good approximation to the actual effective diffusivity if the energy barriers are high enough, but the accuracy of this approximation, at fixed barrier height h, deteriorates as the mobility penalty becomes large and as the cylinders start almost to

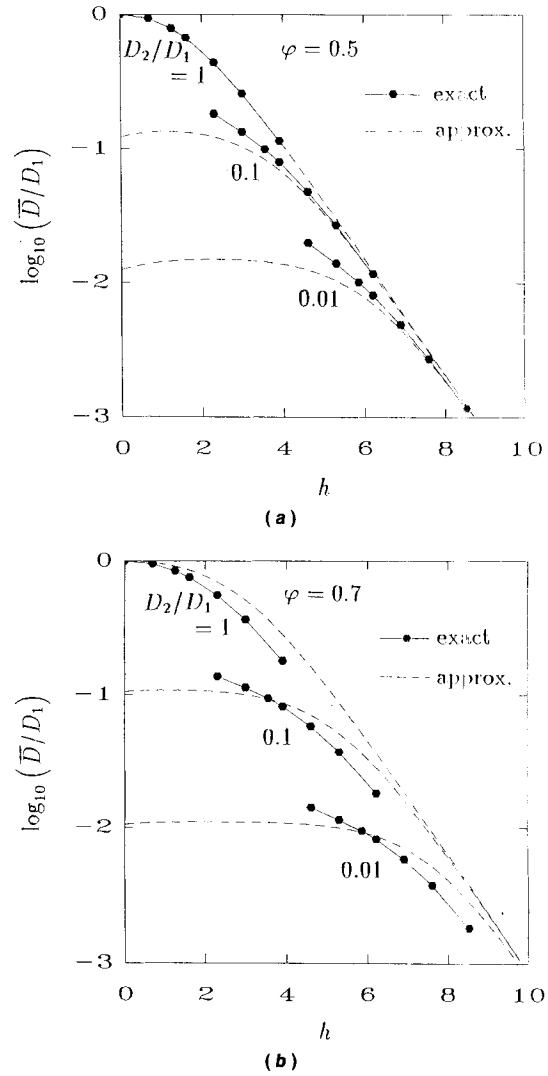

Figure 8. Effective diffusivity as a function of potential variation h and diffusivity ratio D_2/D_1 for the medium shown in Figure 7.

Comparison of exact values derived as stated in Appendix B and approximate values calculated by assuming the one-dimensional, lowest-energy diffusion path I (Eqs. 27 and 28). The circular regions where $\Psi = 0$ occupy area fraction (a) $\varphi = 0.5$, (b) $\varphi = 0.7$.

touch. In view of this numerical example, it seems quite reasonable to speculate that the lowest energy path furnishes a reasonable estimate of the effective diffusivity provided that the corresponding mobility is not too low relative to other possible paths. Further theoretical investigation regarding this point is, of course, in order.

Concluding Remarks

A one-dimensional, phenomenological model has been discussed for configurational diffusion of normal paraffins within zeolite *T*, based on analogies with Brownian motion of a particle over a periodic sequence of energy barriers posed by the throats between the erionite cages. Detailed analysis leads to a semiquantitative description of the "window effect." An 8-carbon paraffin is comparable in length to an erionite cage and can reside in a low-energy state. A 12-carbon paraffin will

extend through a throat into the next cage, so that four of the carbons will reside in a higher-energy state. The activation energy of diffusion would be about 40 kJ/mol for the 8-carbon and zero for the 12-carbon paraffin. Both the postulated activation energies and the diffusivities for 2- to 14-carbon paraffins agree well with experimental values. Future efforts should be directed toward: (1) more detailed understanding of the transport mechanisms for motion of flexible chains (i.e., species with many conformational degrees of freedom) within higher-dimensional heterogeneous structures; and (2) incorporation of more detailed numerical data regarding potential energies for specific molecules contained within zeolites and related materials (cf. June et al., 1990).

Acknowledgment

We would like to thank Dr. R. L. Gorring for providing exact numerical values corresponding to data reported in graphical form in his 1973 article.

Notation

A = variation of $\Phi(x')$
A' = constant additive "background" contribution to $\Phi(x')$
C = unit-cell average paraffin concentration in periodic-potential ("zeolite") medium
C_b = paraffin concentration in bulk solution
$C_1^{[s]}, C_2^{[s]}$ = limiting phase concentrations at surfaces where there is a jump in potential for composite medium in Figure 7
D = diffusivity of aliphatic chain
D_1, D_2 = point-particle diffusivities in two phases of composite medium in Figure 7
$\overline{D}$ = effective diffusivity of chain
D_O = overall steady-state effective diffusivity of chain including partitioning effects
E_a = activation energy in Arrhenius expression for effective diffusivity
$F_b(\lambda; \tau, H)$ = local-maxima-producing factor in effective diffusivity, Eq. 19
$f(\lambda; \tau), g(\lambda; \tau)$ = coefficients appearing in $F_b(\lambda; \tau, H)$
H, H' = dimensionless forms of energy parameters A and A'
h = jump in potential for medium in Figure 7
I_0, I_1 = modified Bessel functions of orders 0 and 1
kT = Boltzmann factor
K = partition coefficient
K_D = phenomenological coefficient in de Gennes-type expression for D
l = period of $\Phi(x')$ and $\Psi(x)$
L = length of aliphatic chain
N = carbon number of normal paraffin
$r(T)$ = pre-exponential factor in Arrhenius expression for effective diffusivity
s = amplitude of potential $\Psi(x)/kT$ for $\Phi(x')$ that varies sinusoidally, Eqs. 11 and 7
x, x' = position coordinates along diffusion path

Greek Letters

α, β, γ = quantities used as labels in the derivation of Eqs. 19–23 in Appendix A and Figure A1
ξ = dimensionless x-coordinate introduced in Appendix A
λ = ratio of chain length L to period of the potential l
φ = volume fraction or area fraction of one phase in a composite medium
$\Phi(x')$ = potential for interaction between normal paraffin and zeolite, in units of energy per unit of paraffin length at position x'
$\Psi(x)$ = total potential energy for interaction between normal paraffin and zeolite when center of paraffin is at position x
τ = parameter giving relative lengths of wells and barriers for periodic step potential

Subscripts

e = erionite
o = offretite
T = zeolite T

Literature Cited

Abramowitz, M., and I. A. Stegun, eds., *Handbook of Mathematical Functions, with Formulas, Graphs, and Mathematical Tables*, 376, Dover, New York (1965).

Barrer, R. M., *Zeolites and Clay Minerals as Sorbents and Molecular Sieves*, Academic Press, New York (1978).

Barrer, R. M., "Sorption by Zeolites: I. Equilibria and Energetics," *Zeolite Science and Technology*, Ribiero, et al., eds., NATO Series E, No. 80, 227 (1984).

Bennett, J. M., and J. A. Gard, "Nonidentity of the Zeolites Erionite and Offretite," *Nature*, **214**, 1005 (1967).

Breck, D. W., *Zeolite Molecular Sieves*, Chap. 1, 77, Wiley, New York (1974).

Brenner, H., and P. M. Adler, "Dispersion Resulting from Flow Through Spatially Periodic Porous Media: II. Surface and Intraparticle Transport," *Phil. Trans. Roy. Soc. Lond.*, Ser. A, **307**, 149 (1982).

Chen, N. Y., S. J. Lucki, and E. B. Mower, "Cage Effect on Product Distribution from Cracking over Crystalline Aluminosilicate Zeolites," *J. Catal.*, **13**, 329 (1969).

Coriell, S. R., and J. L. Jackson, "Potential and Effective Diffusion Constant in a Polyelectrolyte Solution," *J. Chem. Phys.*, **39**, 2418 (1963).

Deen, W. M., "Hindered Transport of Large Molecules in Liquid-Filled Pores," *AIChE J.*, **33**, 1409 (1987).

de Gennes, P. G., "Reptation of a Polymer Chain in the Presence of Fixed Obstacles," *J. Chem. Phys.*, **55**, 572 (1971).

Derouane, E. G., J.-M. Andre, and A. A. Lucas, "Surface Curvature Effects in Physisorption and Catalysis by Microporous Solids and Molecular Sieves," *J. Catal.*, **110**, 58 (1988).

Dieterich, W., P. Fulde, and I. Peschel, "Theoretical Models for Superionic Conductors," *Adv. in Phys.*, **29**, 527 (1980).

Festa, R., and E. Galleani d'Agliano, "Diffusion Coefficient for a Brownian Particle in a Periodic Field of Force: I. Large Friction Limit," *Physica*, **90A**, 229 (1978).

Gorring, R. L., "Diffusion of Normal Paraffins in Zeolite T: Occurrence of Window Effect," *J. Catal.*, **31**, 13 (1973).

Gorring, R. L., personal communication (1991).

Jackson, J. L., and S. R. Coriell, "Effective Diffusion Constant in a Polyelectrolyte Solution," *J. Chem. Phys.*, **38**, 959 (1963).

June, R. L., A. T. Bell, and D. N. Theodorou, "Prediction of Low Occupancy Sorption of Alkanes in Silicalite," *J. Phys. Chem.*, **94**, 1508 (1990).

Kennard, E. H., *Kinetic Theory of Gases, With an Introduction to Statistical Mechanics*, 302, McGraw-Hill, New York (1938).

Larsen, E. W., and Z. Schuss, "Diffusion Tensor for Atomic Migration in Crystals," *Phys. Rev. B*, **18**, 2050 (1978).

Lifson, S., and J. L. Jackson, "On the Self-Diffusion of Ions in a Polyelectrolyte Solution," *J. Chem. Phys.*, **36**, 2410 (1962).

Perrins, W. T., D. R. McKenzie, and R. C. McPhedran, "Transport Properties of Regular Arrays of Cylinders," *Proc. Roy. Soc. Lond.*, Ser. A, **369**, 207 (1979).

Riekert, L., "Sorption, Diffusion, and Catalytic Reaction in Zeolites," *Advances in Catalysis and Related Subjects*, Vol. 21, 281, D. D. Eley, H. Pines, and P. B. Weisz, eds., Academic Press, New York (1970).

Risken, H., *The Fokker-Planck Equation: Methods of Solution and Applications*, 112, Springer-Verlag, New York (1984).

Ruckenstein, E., and P. S. Lee, "Resonant Diffusion," *Phys. Lett.*, **56A**, 423 (1976).

Table A1. Characterization of ψ/kT as a Function of $\xi = xl$ for Various Ranges of λ

Values of λ	Lower Constant Value of Ψ/kT	Assumed on ξ Interval	Higher Constant Value of Ψ/kT	Assumed on ξ Interval(s)
$0 \le \lambda \le 1-\tau$	0	$\lambda/2 \le \xi \le \tau - \lambda/2$	λH	$\tau + \lambda/2 \le \xi \le 1 - \lambda/2$
$1-\tau \le \lambda \le 2(1-\tau)$	As Above	As Above	$(1-\tau)H$	$1-\lambda/2 \le \xi \le \tau - \lambda/2$
$2(1-\tau) \le \lambda \le \tau$	As Above	As Above	As Above	$0 \le \xi \le \tau - 1 + \lambda/2$, $1-\lambda/2 \le \xi \le 1$
$\tau \le \lambda \le 1$	$(\lambda - \tau)H$	$\tau - \lambda/2 \le \xi \le \lambda/2$	As Above	As Above

Schuss, Z., *Theory and Applications of Stochastic Differential Equations*, Chap. 8, Sec. 7, Wiley, New York (1980).

Weaver, D. L., "Note on the Interpretation of Lateral Diffusion Coefficients," *Biophys. J.*, **38**, 311 (1982).

Weisz, P. B., "Zeolites—New Horizons in Catalysis," *Chemtech*, **3**, 498 (1973).

Weisz, P. B., "Molecular Shape Selective Catalysis," *Pure Appl. Chem.*, **52**, 2091 (1980).

Whitaker, S., "Diffusion in Packed Beds of Porous Particles," *AIChE J.*, **34**, 679 (1988).

Appendix A: Derivation of Eqs. 19-23

Attention is focused on values of $\tau \in [2/3, 1]$ and $x \in [0, l]$. It turns out that there are four cases to consider depending on the value of λ. For each case, $\Psi(x)/kT$ assumes one constant value over a prescribed x-interval, a higher constant value over another prescribed x-interval or intervals, and alternates between the two via linear segments of slope $\pm H/l$, as summarized in Table A1 (with $\xi = x/l$ = dimensionless x-coordinate).

The denominator in Eq. 4 is invariant with respect to addition of any constant to the potential, as well as to any horizontal shift of the interval of integration (= one period). Thus, the integrals in Eq. 4 are evaluated most easily by considering $\Psi(x)/kT$ to have the form shown in Figure A1, with parameters α, β and γ given by Table A2. The separate cases $1-\tau \le \lambda \le 2(1-\tau)$ and $2(1-\tau) \le \lambda \le \tau$ have identical representations in terms of α, β, γ, and no longer need be distinguished from one another.

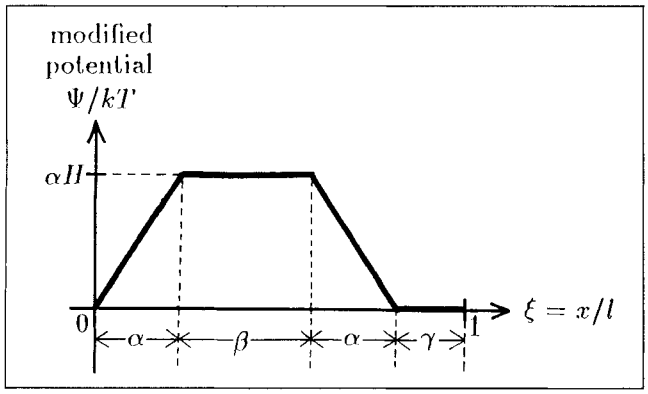

Figure A1. Modified potential energy of aliphatic chain obtained from $\Psi(x)$ via horizontal and (in one case) vertical translation, for substitution into Eq. 4.

Table A2. Parameter Values for Use with Figure A1

λ Interval	α	β	γ
$0 \le \lambda \le 1-\tau$	λ	$1-\tau-\lambda$	$\tau-\lambda$
$1-\tau \le \lambda \le \tau$	$1-\tau$	$\tau+\lambda-1$	$\tau-\lambda$
$\tau \le \lambda \le 1$	$1-\lambda$	$\tau+\lambda-1$	$\lambda-\tau$

Appendix B: Calculation of Effective Diffusivities for the Periodic Medium in Figure 7

A jump in the potential Ψ of magnitude kTh across a surface S, as in Figure 7, leads to a jump condition of the form

$$C_1^{[s]} = KC_2^{[s]}, \tag{B1}$$

with $K = \exp(-h)$, and $C_1^{[s]}$ and $C_2^{[s]}$ the limits of the Brownian particle concentration as one approaches S from the high- and low-potential sides, respectively (cf. Risken, 1984).

Whitaker (1988) has presented an analysis whereby, in present parlance, effective diffusivities for media characterized by a distribution coefficient K can be deduced from effective diffusivities/conductivities of two-phase composites with the same geometry. (Our distribution coefficient K corresponds to the reciprocal of the porosity ϵ_γ in Whitaker's analysis.) The final result to be applied here can be written in the form

$$D_1^{-1}\overline{D}[D_1, D_2, e^{-h}] = (1-\varphi+\varphi e^h)^{-1}\overline{D}[1, (D_2/D_1)e^h, 1], \tag{B2}$$

where $\overline{D}[\sigma_1, \sigma_2, K]$ denotes the effective diffusivity of a composite medium having inclusions (here circular) with diffusivity σ_2 surrounded by a matrix with diffusivity σ_1 and characterized by a distribution coefficient K; φ denotes the area (or volume) fraction of the inclusions (phase 2). Thus, $\overline{D}[D_1, D_2, e^{-h}]$ is the effective diffusivity of the medium in Figure 7; $\overline{D}[1, (D_2/D_1)e^h, 1]$ is the (dimensionless) effective conductivity of a composite with cylinder-phase conductivity $\sigma_2 = (D_2/D_1)e^h$, matrix conductivity $\sigma_1 = 1$, and *equal* distribution between phases ($K = 1$). The "exact" values in Figure 8 follow from the application of Eq. B2 to numerical results for $\overline{D}[1, \sigma_2, 1]$ reported by Perrins et al. (1979). [Note that φ and $\overline{D}[1, \sigma_2, 1]$ correspond to f and ϵ, respectively, in the notation of Perrins et al. (1979).]

Manuscript received Sept. 25, 1990, and revision received Mar. 7, 1991.